# Mutation of an Active Site Residue in *Escherichia coli* Uracil-DNA Glycosylase: Effect on DNA Binding, Uracil Inhibition and Catalysis†

Mary Jane N. Shroyer,‡ Samuel E. Bennett,§ Christopher D. Putnam,|| John A. Tainer,|| and Dale W. Mosbaugh⊥*,§

*Departments of Microbiology, Environmental and Molecular Toxicology, Biochemistry and Biophysics, and the Environmental Health Science Center, Oregon State University, Corvallis, Oregon 97331, and Department of Molecular Biology, Skaggs Institute for Chemical Biology, The Scripps Research Institute, MB4, La Jolla, California 92037*

*Received December 18, 1998; Revised Manuscript Received February 19, 1999*

ABSTRACT: The role of the conserved histidine-187 located in the leucine intercalation loop of *Escherichia coli* uracil-DNA glycosylase (Ung) was investigated. Using site-directed mutagenesis, an Ung H187D mutant protein was created, overproduced, purified to apparent homogeneity, and characterized in comparison to wild-type Ung. The properties of Ung H187D differed from Ung with respect to specific activity, substrate specificity, DNA binding, pH optimum, and inhibition by uracil analogues. Ung H187D exhibited a 55000-fold lower specific activity and a shift in pH optimum from pH 8.0 to 7.0. Under reaction conditions optimal for wild-type Ung (pH 8.0), the substrate preference of Ung H187D on defined single- and double-stranded oligonucleotides (25-mers) containing a site-specific uracil target was U/G-25-mer > U-25-mer > U/A-25-mer. However, Ung H187D processed these same DNA substrates at comparable rates at pH 7.0 and the activity was stimulated ∼3-fold relative to the U-25-mer substrate. Ung H187D was less susceptible than Ung to inhibition by uracil, 6-amino uracil, and 5-fluorouracil. Using UV-catalyzed protein/DNA cross-linking to measure DNA binding affinity, the efficiency of Ung H187D binding to thymine-, uracil-, and apyrimidinic-site-containing DNA was ($dT_{20}$) = ($dT_{19}$−U) ≥ ($dT_{19}$−AP). Comparative analysis of the biochemical properties and the X-ray crystallographic structures of Ung and Ung H187D [Putnam, C. D., Shroyer, M. J. N., Lundquist, A. J., Mol, C. D., Arvai, A. S., Mosbaugh, D. W., and Tainer, J. A. (1999) *J. Mol. Biol. 287*, 331−346] provided insight regarding the role of His-187 in the catalytic mechanism of glycosylic bond cleavage. A novel mechanism is proposed wherein the developing negative charge on the uracil ring and concomitant polarization of the N1−C1′ bond is sustained by resonance effects and hydrogen bonding involving the imidazole side chain of His-187.

Uracil-DNA glycosylase initiates the DNA base excision repair (BER)[1] pathway as a cellular defense mechanism against deamination of cytosine or incorporation of dUMP into DNA (for reviews, see refs *1* and *2*). As the premier enzyme of the BER pathway, uracil-DNA glycosylase specifically recognizes uracil residues in DNA and cleaves the N1−C1′ glycosylic bond between the uracil base and the deoxyribose sugar (*3*, *4*). Recent results suggest that uracil-DNA glycosylase binds, kinks, and compresses the duplex DNA backbone while scanning the minor groove for a uracil residue (*5*). Upon locating the uracil target, the enzyme uses a "push−pull" mechanism to extract the uracil nucleotide from the DNA base stack and position it into the active site (*4*, *6*). This process occurs through a ∼180° rotation of the uracil nucleotide about the phosphodiester backbone resulting in displacement of the uracil residue to an extrahelical position (*4*). This nucleotide-flipping action is essential for substrate recognition and glycosylic bond cleavage. Following the N1−C1′ bond hydrolysis, the enzyme has been shown to utilize a processive search mechanism for locating sequential uracil residues on the same DNA strand (*7*, *8*).

*Escherichia coli* uracil-DNA glycosylase (Ung) is a monomeric, 228 amino acid protein with a deduced molecular weight of 25 694 (*9*, *10*). The enzyme displays ∼2-fold preference for uracil residues located in single-stranded over U/G mispairs in double-stranded DNA, and recognizes U/G mispairs about 2.4-fold more efficiently than U/A basepairs in oligonucleotide substrates (*7*). Ung exhibits catalytic activity over a broad pH range with maximal activity detected at pH 8.0 (*3*). Both free uracil and apyrimidinic sites in DNA inhibit Ung activity by noncompetitive and competitive mechanisms, respectively (*2*, *3*, *11*). *E. coli* uracil-DNA glycosylase shares significant amino acid sequence homology with its counterparts isolated from a wide range of biological

† This work was supported by National Institutes of Health Grants GM32832 and ES00210 to D.W.M. and GM46312 to J.A.T., a National Science Foundation Predoctoral Fellowship to M.J.N.S. and a Howard Hughes Predoctoral Fellowship to C.D.P.

* To whom correspondence should be addressed.

‡ Department of Microbiology, Oregon State University.

§ Department of Environmental and Molecular Toxicology, Oregon State University.

|| Department of Molecular Biology, The Scripps Research Institute.

⊥ Department of Biochemistry and Biophysics and Environmental Health Science Center, Oregon State University.

[1] Abbreviations: BER, base excision repair; Ung, *E. coli* uracil-DNA glycosylase; HSV-1, herpes simplex virus type-1; DTT, dithiothreitol; BSA, bovine serum albumin; bp, base pair(s); IPTG, isopropyl *β*-D-thiogalactopyranoside; EDTA, ethylenediaminetetraacetate adjusted to pH 8.0; SDS, sodium dodecyl sulfate; PAGE, polyacrylamide gel electrophoresis; AP, apurinic/apyrimidinic.

10.1021/bi982986j CCC: $18.00 
Published on Web 03/26/1999

sources including human cells (*5*, *12*, *13*). A comparison of the sequence between *E. coli* Ung and human uracil-DNA glycosylase reveals 55.7% identical residues with 73.3% polypeptide similarity when conservative amino acid substitutions are considered (*12*).

Several lines of evidence have implicated amino acids of *E. coli* Ung that are involved in DNA binding or catalysis. Photochemical cross-linking experiments using Ung and oligonucleotide $dT_{20}$ revealed four tryptic peptides (T6, T18, T19, and T18/19) that adducted to the DNA (*10*). These peptides defined two primary sequences (amino acids 58−80 and 185−213) that reside at or near the DNA-binding site. Amino acid sequence conservation between *E. coli* Ung and 9 other uracil-DNA glycosylases led to speculation that Asp-64 and His-187 serve as essential residues for activity (*10*). Additional insight into the structure and function relationship evolved following the solution of the X-ray crystal structure of herpes simplex virus type-1 (HSV-1) and human Δ84 uracil-DNA glycosylase bound to $dT_3$ and duplex DNA, respectively (*4*, *14*). On the basis of protein structural data, interactions between 13 amino acids and uracil-containing DNA were identified for the human enzyme (*4*). A comparison of the amino acid sequence alignment between *E. coli* and human uracil-DNA glycosylase revealed that *E. coli* Ung possessed 12 (Gln-63, Asp-64, His-67, Phe-77, Ser-88, Asn-123, Ser-166, His-187, Ser-189, Leu-191, Ser-192, and Arg-195) of the same 13 residues attributed to DNA interaction (*4*, *5*). Evidence demonstrating a common role of these amino acids recently emerged from the crystallographic structures of *E. coli* Ung resolved to 3.2 Å (*15*) and 2.4 Å (*16*) resolution. An overlay of the polypeptide Cα traces of human and *E. coli* Ung showed conservation of both secondary-structural elements and tertiary conformation (*15*, *16*). Thus, these results indicate that *E. coli* Ung closely resembles its human enzyme counterpart and that Ung should be regarded as a prototypical enzyme.

Uracil-DNA glycosylase activity requires enzyme-assisted nucleotide flipping to orient the uracil residue within the recognition pocket and to properly position the N1−C1′ bond within the catalytic site (*4*, *14*−*17*). Previously, three different catalytic mechanisms for glycosylic bond cleavage were proposed (*14*, *18*). (1) The peptide carbonyl and side-chain carboxyl of Asp-178 (HSV-1) activate a water molecule that attacks a weakened glycosylic bond. Destabilization of the N1−C1′ bond is brought about by distortion or protonation of the uracil O2 by His-210[2] Nε2 (*14*). (2) The imidazole group of His-268 (human) catalyzes a direct nucleophilic attack on the N1−C1′ glycosylic bond of uracil and a second nucleophilic attack of a water molecule provides H- and OH-group addition to the N1 and C1′ atoms, respectively (*18*). (3) A single nucleophilic attack by His-268 (human) on a water molecule abstracts a proton and creates an OH nucleophile that acts on the glycosylic bond (*18*). In each case, an absolutely conserved histidine residue (human, His-268; HSV-1, His-210) corresponding to *E. coli* Ung His-187 was proposed to play an essential role in catalysis; however, the function of Ung His-187 remains to be fully elucidated.

[2] Originally reported as His-300 from the HSV-1 (strain 17) UL-2 open reading frame that produced cDNA encoding uracil-DNA glycosylase (*13*, *19*−*21*).

In this study, we examine the role of *E. coli* Ung His-187 in mediating catalytic activity. Site-directed mutagenesis was performed on the *E. coli ung* gene producing a H187D mutation. Ung H187D was overproduced, purified, and characterized with regard to specific activity, substrate specificity, DNA-binding affinity, pH optimum, and inhibition by uracil or uracil analogues.

## MATERIALS AND METHODS

*Materials*. Restriction endonucleases (*Bam*HI, *Eco*RI, and *Hin*dIII) were purchased from Life Technologies, and *Bst*XI was purchased from New England Biolabs, as were T4 polynucleotide kinase, T4 DNA polymerase, and T4 DNA ligase. Protein molecular weight markers (SDS-70L) were obtained from Sigma, and poly(U) Sepharose came from Pharmacia Biotech Inc. [$\gamma$-$^{32}$P]ATP was purchased from DuPont-NEN, and [$^3$H]dUTP was from Amersham Corp.

*E. coli* JM105 was provided by W. Ream (Oregon State University), and *E. coli* CJ236 was obtained from T. A. Kunkel (NIEHS). Phagemid pBluescript II SK(−) and VCS-M13 helper phage were supplied by Stratagene. Plasmid pKK223−3 was obtained from Pharmacia Biotech Inc., and pSB1051 was constructed as previously described (*22*). Oligonucleotides were synthesized using an Applied Biosystems 380B DNA Synthesizer by the Center for Gene Research and Biotechnology (Oregon State University). The nucleotide sequence of U-25-mer, A-25-mer, and G-25-mer was previously described (*7*). Oligonucleotides $dT_{20}$ and $dT_{19}$−U, which contained a uracil residue 12 nucleotides from the 5′-end, were prepared as described (*10*). $dT_{19}$−AP was prepared from $dT_{19}$−U by treating with excess *E. coli* uracil-DNA glycosylase. Following excision of >95% of the uracil residues, $dT_{19}$−AP was purified from uracil-DNA glycosylase by Ugi-Sepharose chromatography (*23*) and then concentrated to remove uracil using a Centricon-3 (Amicon) centrifugal concentrator. Deblocked and deprotected oligonucleotides were 5′-end $^{32}$P-labeled as previously described (*10*). Oligonucleotide (42−mer) CTGAAAGCACCGGATCCGTCGCCGCTTTCGGCACATCGTGGA was used for site-directed mutagenesis as described in Figure 1.

*Methods. Site-Directed Mutagenesis of the Ung Gene*. Site-directed mutagenesis to produce Ung H187D was performed as described by Kunkel and co-workers (*24*) with modifications as described by Bennett (*25*). Briefly, the *Bam*HI−*Bam*HI DNA fragment (811 bp) of pSB1051 was inserted into the unique *Bam*HI site of pBluescript II KS(−) using T4 DNA ligase (Figure 1). The resulting phagemid pKS(−)BBUng lacked the nucleotide sequence that coded for the *tac* promoter and the N-terminal 62 amino acids of Ung. *E. coli* CJ236 (*dut*, *ung*) was transformed with pKS(−)BBUng and uracil-containing single-stranded DNA was isolated using VCS-M13 helper phage as described by Lundquist et al. (*21*). Primer extension reactions were carried out using the mutagenic 42-mer deoxyoligonucleotide annealed to uracil-containing single-stranded pKS(−)BBUng DNA according to established procedures (*21*). *E. coli* JM109 was transformed with 10 μL of the primer extension reaction mixture, and plasmid from ampicillin-resistant colonies was isolated, digested with *Bam*HI, and analyzed by 1% agarose gel electrophoresis to identify transformants containing pKS(−)BBUng H187D (Figure 1B).

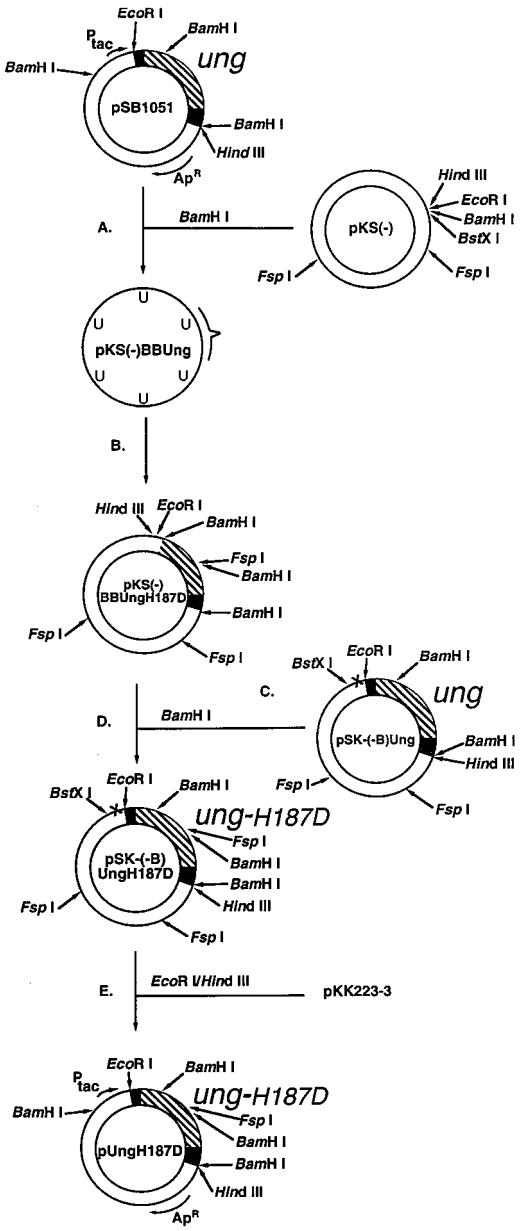


FIGURE 1: Scheme for site-directed mutagenesis of the *E. coli* uracil-DNA glycosylase gene. (A) The pSB1051 *Bam*HI−*Bam*HI restriction fragment (811 bp) containing a portion of the *ung* gene was inserted into the *Bam*HI site of the pKS(−) vector. The resultant construct [pKS(−)BBUng] was transformed into *E. coli* CJ236, and single-stranded DNA rescue was performed to isolate uracil-containing DNA. An oligonucleotide (42-mer) primer was annealed to the single-stranded pKS(−)BBUng DNA template. (B) A primer extension reaction was performed to produce double-stranded pKS(−)BBUng H187D DNA that was used to transform *E. coli* JM109. (C) The *Bam*HI restriction site in the pSK(−) polylinker was removed by digesting with *Bam*HI, filling in the overhanging ends using T4 DNA polymerase, and conducting a blunt-end ligation reaction (former *Bam*HI site denoted by "X"). The *Eco*RI−*Hin*dIII fragment of pSB1051 containing the wild-type *ung* gene was inserted into the pSK(−) derived vector to produce pSK−(−B)-Ung. (D) The *Bam*HI−*Bam*HI restriction fragment containing the wild-type *ung* gene was removed from pSK−(−B)Ung and replaced with the corresponding *ung*H187D fragment from a partial *Bam*HI digest of pKS(−)BBUng H187D to produce pSK−(−B)Ung H187D. (E) The pSK−(−B)Ung H187D *Eco*RI−*Hin*dIII fragment was inserted into the polylinker sites of pKK223−3, placing the *ung*H187D gene under the control of the $p_{tac}$ promoter. DNA manipulations were conducted as described under the Materials and Methods.

*Reassembling the Intact ungH187D Gene*. Before reassembling the *ung*H187D gene, the *Bam*HI recognition site located in the pSK(−) polylinker was removed in a 5′ overhang fill in reaction using T4 DNA polymerase to produce pSK−(−B). The *Eco*RI−*Hin*dIII DNA fragment of pSB1051 encompassing the wild-type *ung* gene was then inserted into the corresponding restriction endonuclease sites of pSK−(−B) to produce pSK−(−B)Ung (Figure 1C). Reassembling the *ung*H187D gene involved the isolation of the *Bam*HI−*Bam*HI−*B*amHI DNA fragment (812 bp) from pKS(−)BBUng H187D by limited digestion. This fragment was then inserted into the *Bam*HI site of pSK−(−B)Ung to produce pSK−(−B)Ung H187D; proper orientation of the insert was verified by restriction endonuclease cleavage with *Fsp*I and *Bst*XI (Figure 1D).

*Construction of the ungH187D Overexpression Plasmid*. The *Eco*RI−*Hin*dIII DNA fragment containing the *ung*H187D structural gene was inserted into the corresponding restriction endonuclease sites of pKK223−3 (Figure 1E). In the resulting construct (pUng H187D), expression of the mutant *ung* gene was under the control of the IPTG-inducible *tac* promoter. The nucleotide sequence of the entire *ung*H187D gene was determined using the dideoxynucleotide chain termination method originally described by Sanger et al. (*26*). DNA sequencing was conducted using an Applied Biosystems model 373A sequencer by the Center for Gene Research and Biotechnology (Oregon State University).

*Purification of Ung and Ung H187D Protein*. *E. coli* uracil-DNA glycosylase (fraction V) was purified from *E. coli* JM105/pSB1051 as previously described by Sanderson and Mosbaugh (*27*). Purification of Ung H187D was similarly conducted through fraction IV with the following modifications: (i) *E. coli* JM109/pUng H187D was grown at 37 °C in 1.25 L of TYN-ampicillin medium; (ii) hydroxyapatite chromatography (fraction IV) was performed using a 10 cm × 2 $cm^2$ column; and (iii) fractions from each column were analyzed by absorbance at 280 nm and by SDS−PAGE. Ung H187D (fraction IV) was dialyzed against DAB buffer [30 mM Tris-HCl (pH 7.4), 1 mM EDTA, 1 mM DTT, and 5% (w/v) glycerol], and one-half of the preparation was applied to a single-stranded DNA agarose column (28 cm × 5.3 $cm^2$) equilibrated in DAB buffer. The column was washed with 150 mL of equilibration buffer and then eluted with 400 mL linear gradient from 0 to 150 mM NaCl in DAB buffer. The flow-through fractions containing Ung H187D were pooled, dialyzed into TMEG buffer [50 mM Tris-HCl (pH 7.5), 10 mM beta-mercaptoethanol, 1 mM EDTA, and 10% (w/v) glycerol], and designated fraction V. Ung H187D (∼8 mg) was applied to a poly(U) Sepharose column (12 cm × 2 $cm^2$) equilibrated in TMEG buffer. The column was washed with 24 mL of equilibration buffer and eluted with 30 mL of TMEG buffer containing 500 mM NaCl. Fractions containing Ung H187D were pooled, concentrated, dialyzed into DAB buffer and designated fraction VI which was used in all characterization experiments.

*Enzyme Assays*. Standard uracil-DNA glycosylase reaction mixtures (100 $\mu$L) contained 70 mM Hepes-KOH (pH 8.0), 1 mM EDTA, 1 mM DTT, 8.2 nmol of calf thymus [*uracil*-$^3$H]DNA (180 cpm/pmol of uracil), and 0.01−0.15 units of *E. coli* uracil-DNA glycosylase. When appropriate, Ung was diluted with UDB buffer containing 50 mM Tris-HCl (pH

8.0), 1 mM EDTA, 1 mM DTT, and 100 μg/mL BSA. Incubation was conducted at 37 °C for 30 min, and the reactions were terminated by addition of 250 μL of 10 mM ammonium formate (pH 4.2) on ice. Free [$^3$H]uracil was resolved from [*uracil*-$^3$H]DNA, and the reaction product was measured by a liquid scintillation spectrometer using 5 mL of Formula 989 (Packard) fluor as described by Bennett and Mosbaugh (*28*). One unit of Ung or Ung H187D is defined as the amount that releases 1 nmol of uracil/h under standard conditions.

Activity on single- and double-stranded [$^{32}$P]U-25-mer substrates was measured in standard reaction mixtures (12.5 μL) containing 70 mM Hepes-KOH (pH 7.0 or 8.0), 1 mM EDTA, 1 mM DTT, 4 pmol of [$^{32}$P]U-25-mer, [$^{32}$P]U/A-25-mer or [$^{32}$P]U/G-25-mer (15500−22000 cpm/pmol), and various amounts of Ung or Ung H187D as indicated in the figure legends. After incubations for 30 min at 37 °C, the reactions were terminated on ice with 0.8 mg of uracil-DNA glycosylase inhibitor protein. Apyrimidinic sites were hydrolyzed by addition of 3 M $K_2HPO_4$ (pH 13.7) to 10% (v/v) and incubation at 55 °C for 3 h. Following the hydrolysis reaction, samples were neutralized with 3 μL of 1.5 M $KH_2PO_4$ and combined with 17.5 μL of denaturing sample buffer (95% deionized formamide, 10 mM EDTA, 0.1% bromphenol blue, and 0.1% xylene cyanol). After heating at 95 °C for 3 min, samples (10 μL) were then examined by 12% urea−polyacrylamide gel electrophoresis.

*Ung/DNA-Binding Assay*. Ung and Ung H187D binding to DNA was measured using a modified procedure of that described by Molnar et al. (*29*). Standard binding reaction mixtures (15 μL) contained either Ung or Ung H187D and various 5′-end $^{32}$P-labeled oligonucleotides in DAB buffer as indicated in the figure legends. Samples were placed into a 96 well microtiter plate (Corning round-bottom well, low protein binding), incubated for 15 min on ice, and UV irradiated ($\lambda_{max}$ = 254 nm) for 30 min in a Stratalinker 1800 (Stratagene Cloning Systems). Following the UV-catalyzed cross-linking reaction, samples (25 μL) were analyzed by 12.5% SDS−PAGE as described by Bennett et al. (*10*). After electrophoresis, the lower part of the gel containing un-cross-linked [$^{32}$P]oligonucleotide was removed to reduce background radioactivity. Gels were stained with Coomassie Brilliant Blue G-250, dried, and Ung × [$^{32}$P]DNA cross-linked material detected by autoradiography. The amount of Ung × [$^{32}$P]DNA was quantified by excising the bands, solubilizing the gel, and measuring the $^{32}$P radioactivity in a liquid scintillation counter (*27*).

*Polyacrylamide Gel Electrophoresis*. SDS−polyacrylamide slab gel electrophoresis was performed essentially as described by Laemmli (*30*) and modified by Bennett et al. (*10*). DNA sequencing gels containing 12% acrylamide, 0.41% *N*,*N*′-methylenebis (acrylamide), 8.3 M urea, and TBE buffer (90 mM Tris base, 90 mM boric acid, and 2 mM EDTA) were used to analyze the uracil-DNA glycosylase reaction products produced from 5′-end $^{32}$P-labeled oligonucleotide substrates (*7*).

*Protein Measurements*. Protein concentrations of crude extracts were determined by the Bradford reaction (*31*) using the Bio-Rad assay. Purified protein concentrations were determined by absorbance spectroscopy using the molar extinction coefficients $\epsilon_{280\ nm} = 4.2 \times 10^4$ L/mol cm (Ung, Ung H187D) and $\epsilon_{280\ nm} = 1.2 \times 10^4$ L/mol cm (Ugi) as previously described (*10*).

## RESULTS

*Site-Directed Mutagenesis of the E. coli Uracil-DNA Glycosylase Gene*. To investigate the function of Ung His-187 in DNA-binding and catalysis, site-directed mutagenesis of the *E. coli ung* gene was performed as described in Figure 1. The approach utilized the oligonucleotide-directed mutagenesis strategy developed by Kunkel and co-workers (*24*). Since this cloning method depends on propagating phagemid DNA containing the target gene (*ung*) in *E. coli* CJ236 (*dut*$^-$, *ung*$^-$) cells, it was necessary to perform mutagenesis using a *Bam*HI fragment of the *ung* gene rather than the full-length gene that would otherwise confer uracil-DNA glycosylase activity to the bacterial cells. A strategy was devised for creating a single amino acid substitution that converted His-187 to aspartic acid. First, the *Bam*HI restriction fragment of pSB1051 which lacked the nucleotide sequence encoding the N-terminal 62 amino acids of Ung was subcloned into pKS(−) DNA to produce pKS(−)BBUng, and uracil-containing single-stranded DNA was isolated from transfected *E. coli* CJ236 cells (Figure 1A). Second, an oligonucleotide primer (42-mer) was annealed to pKS(−)BBUng, and primer extension was carried out (Figure 1B). This oligonucleotide introduced a C to G transversion mutation into the His-187 codon (CAT) that produced both an amino acid substitution to Asp (GAT) and a new *Bam*HI restriction endonuclease site that facilitated detection of the mutation. Third, the *Bam*HI site located in the pSK(−) polylinker region was eliminated producing pSK−(−B)Ung which facilitated the reassembly of the full-length *ung* gene (Figure 1, panels C and D). Fourth, the *Eco*RI−*Hin*dIII DNA fragment of pSK−(−B)Ung H187D was subcloned into the overexpression vector pKK223−3 producing pUng H187D with the mutant *ung* gene under the control of the *tac* promoter (Figure 1E). The *ung*H187D gene was completely sequenced, and the results indicated that only the desired amino acid substitution (H187D) had been introduced during site-directed mutagenesis (*25*).

*Overproduction and Purification of the Ung H187D Protein*. Attempts to transform pUng H187D into *E. coli* BD2314 and BW310 (*ung*$^-$ strains) proved unsuccessful because the vector was found to be unstable. In contrast, pUng H187D was successfully transformed into *E. coli* JM105, an *ung*$^+$ strain, for overproduction of Ung H187D protein. To assess the level of Ung H187D overproduction, three mid-log cultures of *E. coli* JM105 cells transformed with either pKK223−3 (vector control), pSB1051 (*ung* overexpression vector), or pUng H187D (*ung*H187D overexpression vector) were each divided in half and grown in the presence or absence of 1 mM IPTG to induce *ung* gene expression. Cell-free extracts were analyzed by 12.5% SDS−PAGE as shown in Figure 2. A Coomassie Brilliant Blue stainable protein band corresponding to the approximate molecular weight of Ung ($M_r$ = 25 000) was found to be IPTG-induced in *E. coli* containing pSB1051 (Figure 2, lane 4) and pUng H187D (Figure 2, lane 6). Using scanning densitometry, we estimated that Ung represented ∼13% and Ung H187D comprised ∼18% of the total soluble cell protein following overproduction.

The specific activity of uracil-DNA glycosylase was determined for each cell-free extract (Figure 2). As expected, *E. coli* JM105 cells transformed with pSB1051 displayed

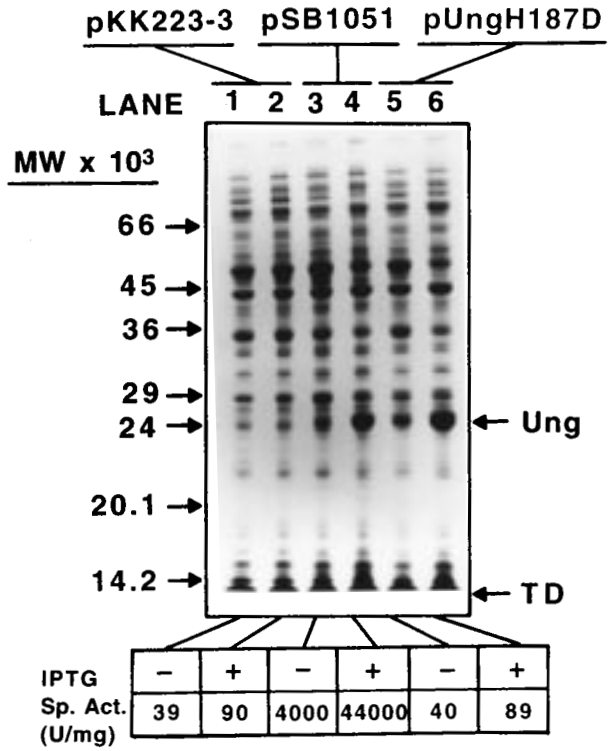


FIGURE 2: Overproduction of Ung H187D from pUng H187D. *E. coli* JM105 transformed with pKK223−3 (lanes 1 and 2), pSB1051 (lanes 3 and 4), or pUng H187D (lanes 5 and 6) were grown in the presence (+) or absence (−) of 1 mM IPTG as indicated. Cell-free extracts were prepared, samples (25 $\mu$g of total protein) were analyzed on a 12.5% polyacrylamide gel containing SDS, and protein bands were visualized after staining with Coomassie Brilliant Blue G-250 as described under Materials and Methods. The molecular weight standards for bovine serum albumin, ovalbumin, glyceraldehyde-3-phosphate dehydrogenase, carbonic anhydrase, trypsinogen, trypsin inhibitor and α-lactalbumin are indicated by arrows from top to bottom, respectively. The location of the tracking dye (TD) and Ung are shown by arrows. The specific activity of uracil-DNA glycosylase in each cell-free extract was determined using standard assay conditions.

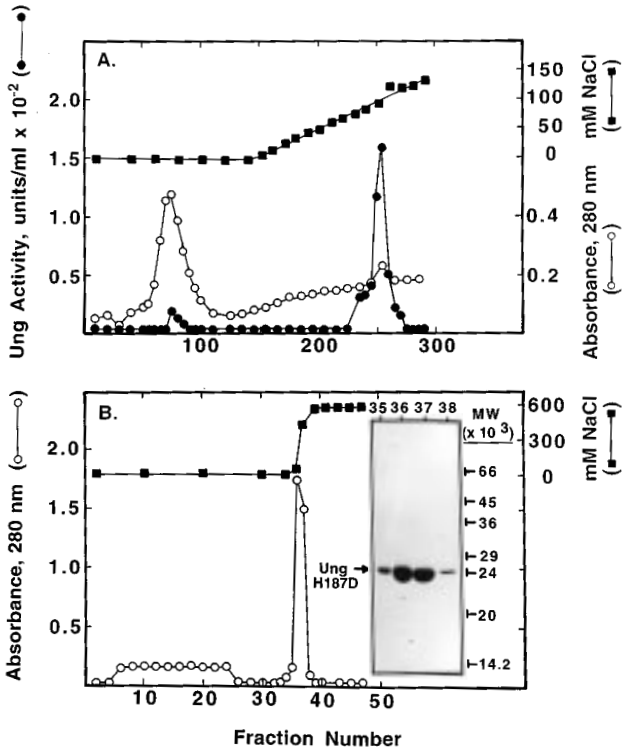


FIGURE 3: Purification of Ung H187D using single-stranded DNA agarose and poly(U) Sepharose chromatography. Ung H187D (Fraction IV) was purified as described under the Materials and Methods. (A) Ung H187D (fraction IV, 17 mg) was dialyzed against DAB buffer and applied to a single-stranded DNA agarose column equilibrated with DAB buffer. The column was then washed and eluted with a linear gradient of 0 to 150 mM NaCl in DAB buffer (■). Fractions (2.5 mL) were collected, 25 $\mu$L aliquots were used to assay for Ung activity (●), and the absorbance ($OD_{280nm}$) of samples were measured (○). Flow-through fractions (62−102) were pooled and dialyzed against TMEG buffer. (B) After dialysis, Ung H187D (fraction V, 8 mg) was loaded onto a poly(U) Sepharose column equilibrated with TMEG buffer. The column was washed and eluted stepwise with 500 mM NaCl in TMEG buffer. Fractions (2 mL) were collected and the absorbance at 280 nm measured (○). Peak fractions (35−38) were analyzed on a 12.5% polyacrylamide gel containing SDS (insert) as described in Figure 2. The location of Ung H187D is indicated by an arrow.

an IPTG-inducible Ung activity. Overproduction of Ung in *E. coli* JM105/pSB1051 cells produced 44 000 units/mg of cellular protein, which was 11-fold higher than that of uninduced cells and ∼1100-fold higher than cells containing the vector control. In contrast, *E. coli* JM105/pUng H187D cells treated with or without IPTG did not show increased specific activity of uracil-DNA glycosylase relative to the cells containing the vector control (pKK223−3). In each case, the specific activity was essentially equivalent to that of the corresponding vector only control, though the Ung H187D protein was overproduced. These results implied that the Ung H187D protein was defective in uracil-DNA glycosylase activity.

To facilitate characterization of Ung H187D, the protein was overproduced in *E. coli* JM105/pUng H187D and purified according to the procedure of Sanderson and Mosbaugh (*27*). During the purification (fractions I−IV), a relatively small amount of uracil-DNA glycosylase activity copurified with the overproduced Ung H187D protein of ∼25 000 molecular weight (data not shown). However, upon chromatography of Ung H187D (fraction IV) on a single-stranded DNA agarose column two peaks of Ung activity were detected (Figure 3A). The major activity peak containing a relatively small amount of protein eluted from the column matrix at a NaCl concentration (∼100 mM) characteristic of wild-type Ung. The minor activity peak found in the flow-through fractions constituted ∼9% of the recovered activity but contained a relatively large amount of protein. Analysis of the flow-through fractions using SDS−PAGE revealed a large protein band ($M_r \approx 25\,000$) corresponding to the overproduced Ung H187D protein and several minor contaminants. Additional purification of Ung H187D was carried out using a poly(U) Sepharose column (Figure 3B). Ung H187D which bound to the matrix was stepwise eluted producing an apparently homogeneous preparation (Figure 3B, insert). After pooling the peak fractions, the specific activity of Ung H187D was determined to be 37 units/mg, whereas wild-type Ung has a specific activity of $2.1 \times 10^6$ units/mg under standard reaction conditions (*22*).

*Rechromatography of Ung H187D on Single-Stranded DNA Agarose*. Although single-stranded DNA agarose chromatography appeared to separate Ung H187D from wild-type Ung (Figure 3A), this observation alone did not eliminate the possibility that the activity detected in the Ung H187D preparation was due to a trace contaminant of Ung.

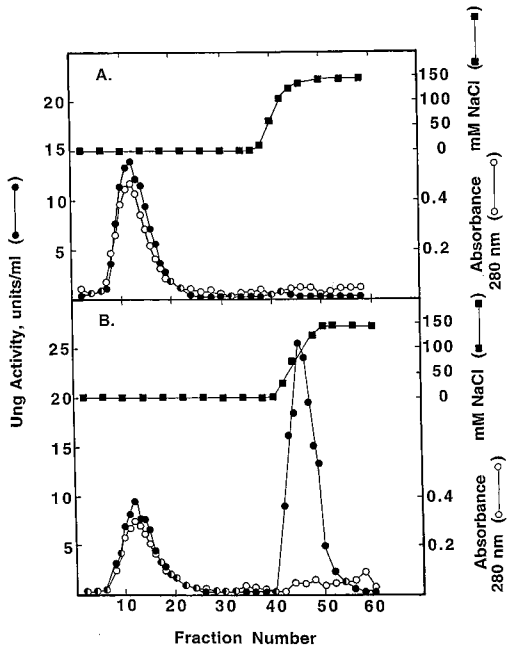


FIGURE 4: Rechromatography of Ung H187D on single-stranded DNA agarose. (A) Ung H187D (fraction VI, 167 units) was applied to a single-stranded DNA agarose column (5.7 cm × 1.8 cm$^2$) equilibrated in DAB buffer. The column was washed and then step-eluted with DAB buffer containing 150 mM NaCl. (B) A sample containing Ung H187D (fraction VI, 167 units) and wild-type Ung (fraction V, 167 units) in DAB buffer was prepared and single-stranded DNA agarose chromatography performed as described in panel A. Fractions (1 mL) were collected, assayed for uracil-DNA glycosylase activity (●), measured for absorbance at 280 nm (○), and monitored for conductivity (■).

To determine if residual Ung was present in Ung H187D (fraction VI), a sample (167 units) of Ung H187D was rechromatographed on a single-stranded DNA agarose column (Figure 4A). A single peak of activity was detected in the flow-through fractions and no significant activity was observed binding to the matrix with characteristics of wild-type Ung. To verify that this chromatographic system would have resolved an Ung contaminant, if present, the experiment was repeated using an identical sample of Ung H187D to which 167 units of Ung was added. Following chromatography, two peaks of activity corresponding to Ung H187D and Ung were resolved and the specific activity of Ung H187D in the flow-through fractions was essentially unchanged (Figure 4B). Together these observations suggest that the activity detected in the Ung H187D preparation was inherent to the mutant enzyme.

*pH Optimum of Ung H187D Activity*. The specific activity of Ung H187D and Ung was determined in Tris-HCl and Hepes-KOH buffers over a pH range of 6.5−9.5 (Figure 5). Maximal activity of Ung H187D was observed with Hepes-KOH at pH 7.0, which was one pH unit less than the pH optimum for Ung (pH 8.0).

*Substrate Specificity*. The relative ability of Ung and Ung H187D to remove uracil from either a single-stranded or double-stranded oligonucleotide containing a U/A base paired or U/G mispaired site was examined. A 5′-end $^{32}$P-labeled oligonucleotide ([$^{32}$P]U-25-mer) with a site-specific uracil residue at position 11 was annealed to one of two complimentary oligonucleotides producing either a [$^{32}$P]U/A-25-mer or a [$^{32}$P]U/G-25-mer DNA substrate. The single- or

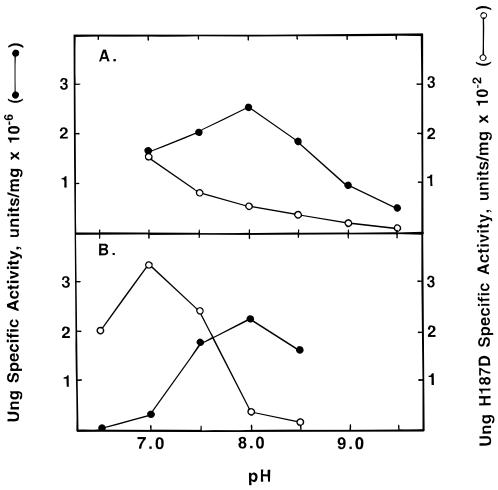


FIGURE 5: Comparison of pH optima of wild-type Ung and Ung H187D activity. Four sets of standard uracil-DNA glycosylase reaction mixtures containing Ung (●) or Ung H187D (○) were prepared except that either (A) 70 mM Tris-HCl (pH 7.0−9.5) or (B) 70 mM Hepes-KOH (pH 6.5−8.5) was used as a buffer as indicated above. Three concentrations (0.03−0.13 units) of enzyme were assayed at each pH and used to determine the specific activity for each reaction condition.

double-stranded nature of the three substrates was verified following nondenaturing polyacrylamide gel electrophoresis as described by Bennett et al. (*7*). Each of the three substrates (U, U/A, and U/G) were incubated with Ung at pH 8.0 to catalyze uracil excisions producing apyrimidinic sites. After alkali-induced cleavage of the deoxyribose-phosphate bond, an AP-site containing [$^{32}$P]11-mer was resolved by denaturing polyacrylamide gel electrophoresis as the reaction product (Figure 6, panels A−C, respectively). The rate of uracil excision was determined for each DNA substrate, and the wild-type Ung was found to hydrolyze the single-stranded U-25-mer about 3- and 5-fold faster than the U/G- and U/A-25-mer, respectively. Interestingly, when Ung H187D was examined under the same reaction conditions, the U/G-25-mer was found to be the preferred substrate. Activity on the single-stranded U-25-mer and the U/A-25-mer was reduced by ∼1.5- and 2.3-fold, respectively, compared to the U/G-25-mer substrate (Figure 6, E−H). When Ung H187D was assayed at its optimal pH of 7.0, all three substrates were processed with similar efficiencies (data not shown). Activity on the U/G- and U/A-25-mer was determined to be 75 and 86% of the rate of activity on the U-25-mer, which was increased ∼3-fold relative to the assay at pH 8.0.

*Effect of Uracil on Ung and Ung H187D Activity*. Inhibition studies were conducted to determine whether the H187D mutation of Ung affected the binding of uracil to the enzyme. Standard assays were conducted using Ung or Ung H187D in the presence of various amounts of free uracil, 6-amino uracil, or 5-fluorouracil and the percent of activity relative to the control was determined as shown in Figure 7. At pH 8.0, Ung activity appeared to be 50% inhibited by ∼0.15 mM uracil. In contrast, Ung H187D was much more resistant and showed about 7.5% inhibition at the same uracil concentration. Similar results for inhibition by uracil were observed for reactions conducted at pH 7.0 (Figure 7A). Substitution of 6-amino uracil in place of uracil also demonstrated that Ung was more sensitive to the inhibitor than Ung H187D, and that the observed level of inhibition

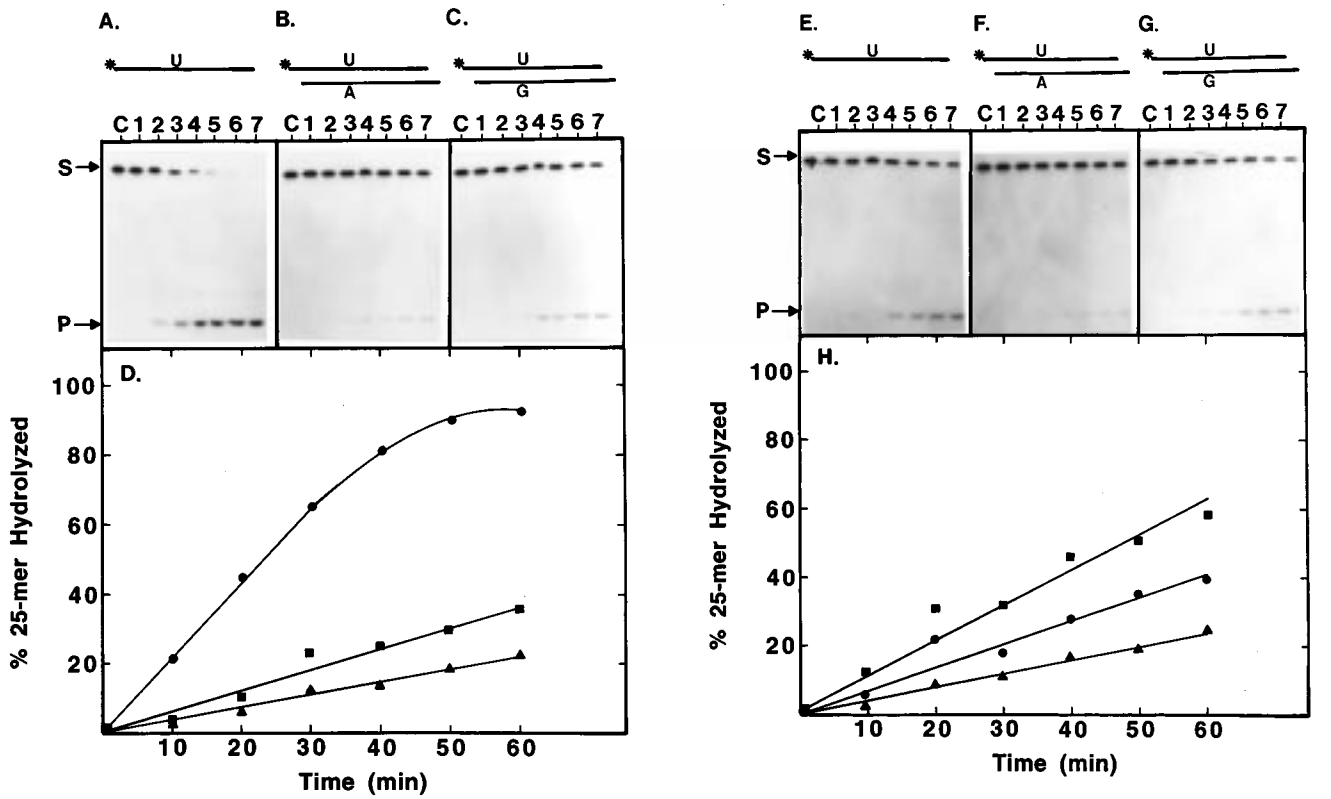


FIGURE 6: Substrate specificity of Ung and Ung H187D. Three sets of standard uracil-DNA glycosylase reaction mixtures (125 $\mu$L) each containing 0.3 units of Ung and either [$^{32}$P]U-25-mer (A), [$^{32}$P]U/A-25-mer (B), or [$^{32}$P]U/G-25-mer (C) were incubated at 37 °C for 0, 10, 20, 30, 40, 50, and 60 min (lanes 1−7, respectively). Reactions were conducted using 70 mM Hepes-KOH (pH 8.0) as a buffer. A control reaction (lane C) was prepared which was incubated without Ung on ice for 60 min. After incubation, each reaction was terminated, AP sites were hydrolyzed by alkaline treatment, and samples were analyzed using denaturing 12% urea-polyacrylamide gel electrophoresis as described under Materials and Methods. Arrows indicate the locations of 25-mer substrate (S) and 11-mer product (P) on the autoradiogram. (D) Radioactive bands were excised from the dried gel, the amount of $^{32}$P radioactivity was measured for bands S and P, and the percent of 25-mer hydrolyzed for the U (●)-, U/A (▲)-, and U/G (■)-containing oligonucleotide was calculated as previously described (*7*). Three similar sets of reaction mixtures each containing Ung H187D and either [$^{32}$P]U-25-mer (E), [$^{32}$P]U/A-25-mer (F), or [$^{32}$P]U/G-25-mer (G) were incubated. (H) The percent of 25-mer hydrolyzed for each substrate was determined as described above.

was not significantly affected by the change of pH (Figure 7B). Inhibition of Ung by 5-fluorouracil (Figure 7C) was least pronounced, regardless of pH: ∼20% at 1 mM 5-fluorouracil. Moreover, inhibition of Ung H187D was not observed at any of the 5-fluorouracil concentrations tested (Figure 7C).

*Ability of Ung and Ung H187D to Bind DNA.* To assess the relative affinity of Ung and Ung H187D for DNA, UV-catalyzed cross-linking experiments were conducted using three different oligonucleotides. Nonspecific DNA interactions were analyzed after mixing [$^{32}$P]$dT_{20}$ with either Ung or Ung H187D, irradiating with UV-light for various times, and resolving the reaction products using SDS−PAGE. Autoradiography was used to detect the enzyme × [$^{32}$P]$dT_{20}$ bands as shown in Figure 8A. The rate of cross-linking was determined by measuring the amount of $^{32}$P radioactivity contained in the enzyme × $dT_{20}$ bands as a function of UV irradiation time (Figure 8B). A comparison of the cross-linking rates indicated that Ung (0.36 pmol/min) was ∼2.2-fold more efficient than Ung H187D (0.16 pmol/min) at forming a protein × $dT_{20}$ complex. Enzyme saturation experiments using various concentrations of oligonucleotide to perform UV-catalyzed cross-linking revealed the extent of Ung and Ung H187D × $dT_{20}$ product formation (Figure 9A). In both cases, cross-linking increased with increasing $dT_{20}$ concentration until reaching a plateau where ∼1.5-fold more Ung × $dT_{20}$ than Ung H187D × $dT_{20}$ was produced. The experiment was also conducted using [$^{32}$P]$dT_{19}$−U, a uracil-containing oligonucleotide (20-mer) possessing a uracil residue 12 nucleotides from the 5′-end (Figure 9B). Using this DNA substrate, the ability of Ung H187D, relative to Ung, to form a cross-linked complex was nearly identical. In addition, the cross-linking efficiency was measured using [$^{32}$P]$dT_{19}$−AP, which contained an apyrimidinic site in place of the site-specific uracil residue of $dT_{19}$−U (Figure 9C). Recognition of $dT_{19}$−AP by Ung was ∼2-fold greater than by Ung H187D, due primarily to the decreased ability of Ung H187D to cross-link to this oligonucleotide relative to either $dT_{20}$ or $dT_{19}$−U.

*Effect of Uracil on DNA Binding.* To determine the effect of free uracil on the DNA affinity of Ung and Ung H187D, UV-catalyzed cross-linking experiments were carried out in the presence of [$^{32}$P]$dT_{20}$ and 2 mM uracil (Figure 10). Inspection of the respective autoradiographs (Figure 10, panels A and B) and cross-linking rates (Figure 10C) shows that, in the absence of uracil, the extent of UV-catalyzed oligonucleotide cross-linking to Ung was approximately twice that of Ung H187D. However, in the presence of the highly inhibitory concentration of free uracil, the extent of Ung cross-linking remained unaffected, whereas Ung H187D cross-linking was reduced greater than 2-fold.

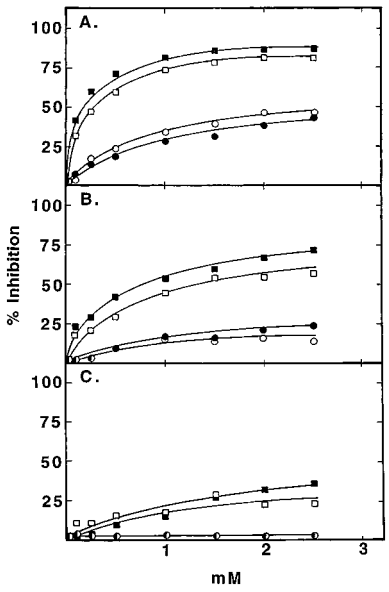


FIGURE 7: Effect of uracil on wild-type Ung and Ung H187D activity. (A) Four sets of standard uracil-DNA glycosylase reaction mixtures (100 $\mu$L) were prepared containing either 1.3 units of Ung (□, ■) or 0.6 units of Ung H187D (○, ●). Reactions were conducted using 70 mM Hepes-KOH (pH 8.0) (■, ●) or 70 mM Hepes-KOH (pH 7.0) (□, ○) and each reaction was supplemented with various amounts of uracil as indicated. (B) Similarly, four sets of reaction mixtures were prepared and supplemented with different amounts of 6-amino uracil or (C) 5-fluorouracil as indicated. After incubation at 37 °C for 30 min, the amount of [$^3$H]uracil released from the DNA substrate was measured. The percent of Ung activity inhibited was determined relative to the control lacking uracil.

## DISCUSSION

We have used site-directed mutagenesis to examine the role of an active-site amino acid residue (His-187) in uracil-DNA recognition and excision by *E. coli* uracil-DNA glycosylase. Recently, the structures of both Ung and Ung H187D in complex with the uracil-DNA glycosylase inhibitor protein were determined by X-ray crystallography, at 2.4 and 2.6 Å resolution, respectively (*16*). Ung is the first full-length uracil-DNA glycosylase for which crystal structure information is available (*15*, *16*). Overlay of the Ung and Ung H187D structures indicated that the mutant protein is properly folded with respect to the wild-type enzyme, and the principal amino acid residues that form the uracil-binding pocket and active site (Asp-64, Pro-65, Tyr-66, Phe-77, Asn-123, and His/Asp-187) of Ung and Ung H187D are nearly superimposable when the two structures are compared (*16*). Moreover, structural comparison of *E. coli* Ung with both the human (*17*) and HSV-1 (*32*) uracil-DNA glycosylase homologues have indicated that the major structural motifs implicated in enzyme function and specificity have been conserved (*15*, *16*). Thus, conclusions concerning the catalytic role of Ung His-187 are most likely applicable to the various members of the uracil-DNA glycosylase protein family for which this amino acid is an absolutely conserved residue.

During the purification of overexpressed Ung H187D, we observed that, unlike the endogenous wild-type enzyme, the H187D mutant failed to bind single-stranded DNA agarose under conditions conducive to stable binding by wild-type Ung. In contrast, Ung H187D was observed to stably bind to poly(U) Sepharose. This finding indicated that the His to

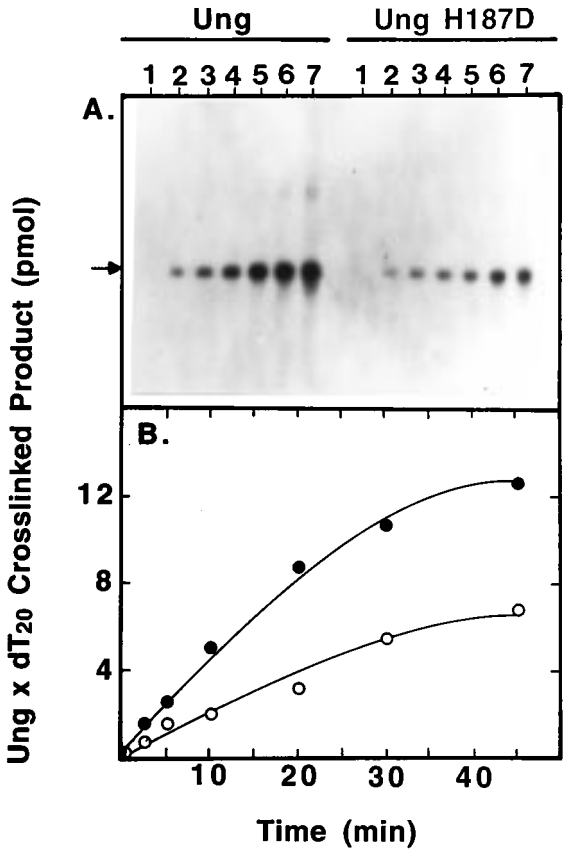


FIGURE 8: Relative ability of Ung and Ung H187D to form UV-catalyzed cross-links with $dT_{20}$. (A) Two reaction mixtures (150 $\mu$L) containing DAB buffer, 7.6 nmol of either Ung or Ung H187D were UV-irradiated on ice as described under Materials and Methods. At the times indicated below, 15 $\mu$L samples were removed and analyzed by 12.5% SDS−PAGE. The protein bands were visualized after Coomassie Brilliant Blue G-250 staining and the enzyme x [$^{32}$P]$dT_{20}$ (arrow) was detected by autoradiography. Lanes 1−7 correspond to UV exposure times of 0, 2.5, 5, 10, 20, 30, and 45 min, respectively. (B) The amount of [$^{32}$P]$dT_{20}$ cross-linked to Ung (●) and Ung H187D (○) was quantitated by excising the radioactive bands from the dried gel, solubilizing the gel with 30% $H_2O_2$ at 55 °C, and measuring the $^{32}$P radioactivity in a liquid scintillation counter using 5 mL of Formula 989 fluor.

Asp substitution abrogated the ability of the mutant enzyme to form a persistent complex with single-stranded DNA. However, we infer both from the low catalytic activity and from the observed inhibition by free uracil that Ung H187D conserved, to some extent, the native uracil nucleotide interaction. A structural comparison of the active sites implies that steric constraints should not dramatically affect uracil binding by Ung H187D (Figure 11). Furthermore, the experimental findings indicating altered DNA substrate specificity of Ung H187D suggested that the negative charge of the Asp-187 side chain may repel the phosphate backbone of the single-stranded DNA, which is less constrained than in double-stranded DNA. This interpretation was consistent with the close proximity of the Asp-187 carboxyl group to the 3′- and 5′-phosphates of the target uracil nucleotide in DNA (Figure 11B). In addition, when the equivalent histidine residue in human uracil-DNA glycosylase (His-268) was mutated to Leu, significantly lowered affinity to DNA was not observed (*18*), presumably because the Leu side chain lacked the long-range interactions of the Ung Asp-187 carboxylate. In the case of poly(U) binding, perhaps the

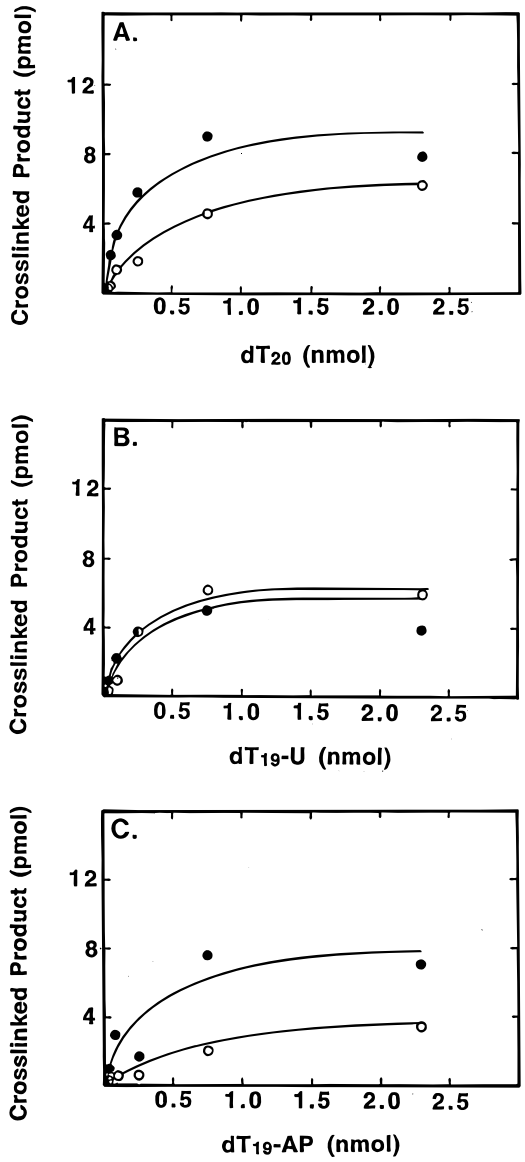


FIGURE 9: Effect of uracil- and AP-sites on UV-catalyzed cross-linking of Ung and Ung H187D to $dT_{20}$. (A) Samples (15 $\mu$L) containing 0.38 nmol of Ung (●) or Ung H187D (○) and 0.028, 0.084, 0.25, 0.76, or 2.28 nmol of [$^{32}$P]$dT_{20}$ were UV irradiated for 30 min as described under Materials and Methods. Identical UV-catalyzed cross-linking reactions were carried out except that [$^{32}$P]$dT_{19}$−U (B) or [$^{32}$P]$dT_{19}$−AP (C) was substituted as the oligonucleotide. After UV irradiation, samples were analyzed by 12.5% SDS−PAGE and the amount of enzyme cross-linked to [$^{32}$P]-oligonucleotide was determined by liquid scintillation counting as described in Figure 8.

negative Asp-187 carboxylate:phosphate interaction in DNA is mitigated in part by hydrogen bonding between the ribose 2′ hydroxyl and the Asp side chain.

*E. coli* Ung was purified to apparent homogeneity, and a low level of uracil-DNA glycosylase activity was detected in the Ung H187D preparation. This activity was reduced approximately 55000-fold relative to that of wild-type Ung as indicated by a specific activity of 37 units/mg. On the basis of this observation, Ung H187D was calculated to have a turnover rate of 0.95 uracil/h. Several observations indicated that the activity of the Ung H187D preparation was inherent to the mutant protein and not the result of very low-level contamination by cellular Ung: (1) a preparation of Ung H187D deliberately contaminated with Ung was effectively resolved into two distinct peaks (mutant and wild-type Ung) using DNA-agarose affinity chromatography, which was applied to the separation procedure during the final step in the purification protocol; (2) the pH optimum of Ung H187D (pH 7.0) was distinct from that of Ung (pH 8.0); and (3) the substrate specificity of Ung H187D differed from that of Ung. From these observations, we concluded that the H187D mutant enzyme preparation was sufficiently pure to warrant further characterization.

As previously shown, uracil-DNA glycosylases display a marked preference for single-stranded uracil-containing DNA and favor U/G mispairs over U/A base pairs in double-stranded DNA (*7*, *33*). Under conditions optimal for wild-type Ung (pH 8.0), the substrate preference of Ung H187D was U/G-25-mer > single-stranded U-25-mer > U/A-25-mer. However, at pH 7.0 Ung H187D processed these same DNA substrates at comparable rates, although single-stranded U-25-mer was slightly preferred. Furthermore, activity on the single-stranded uracil-DNA substrate increased about 3-fold at pH 7.0 compared to that at pH 8.0. That the substrate specificity and specific activity of Ung H187D were pH-dependent suggested that the protonation state of the Asp-187 $\gamma$-carboxylate may affect various aspects of the uracil-excision reaction including the extent and duration of DNA binding, uracil nucleotide flipping, and stabilization of the uracil/deoxyribose transition state. In this regard, it was interesting to note that the effect of pH on uracil inhibition of both Ung and Ung H187D was small, and that Ung H187D was less susceptible than Ung to uracil inhibition. In addition, the mutant enzyme was not inhibited by 5-fluorouracil at any of the concentrations tested. Taken together, these results imply that the Asp mutation reduced the affinity of the active site for uracil. This can be explained from a structural basis as caused by loss of hydrogen bonding and repulsive electrostatic interactions with the permanent electric dipole at uracil O2 (Figure 11). In the case of 5-fluorouracil, steric interference and like-charge repulsion by the 5-fluorine moiety with the Asp187 side chain were apparently sufficient to preclude binding. Conversely, one might expect that nonpolar substitutions at residue 187, such as Leu, would not affect 5-fluorouracil inhibition.

Using UV-catalyzed protein/DNA cross-linking as a measure of DNA binding affinity, we determined that the efficiency of Ung His-187 cross-linking to the oligonucleotide $dT_{20}$ was about the same as to $dT_{19}$−U. Thus, the presence of uracil in the 20-mer did not increase the DNA-binding affinity of Ung H187D. Since the turnover rate of the Ung H187D mutant was very low (∼1 uracil/h), it seemed unlikely that very many AP-sites were created during the 30 min UV irradiation. Moreover, the extent of UV-catalyzed cross-linking to an AP-site-containing oligonucleotide ($dT_{19}$−AP) was reduced about 50% relative to the rate on $dT_{19}$−U. These results suggested that the main factor affecting the uracil-DNA binding affinity of Ung H187D was not the recognition of uracil but the Asp-187 $\gamma$-carboxylate/DNA phosphate electrostatic repulsion. We speculate that the negative electrostatic interaction was probably more pronounced when the DNA substrate contained an abasic site, as the 3′- and 5′-deoxyribose phosphates were more accessible.

Unexpectedly, the wild-type enzyme was cross-linked by UV irradiation less efficiently to the uracil-containing

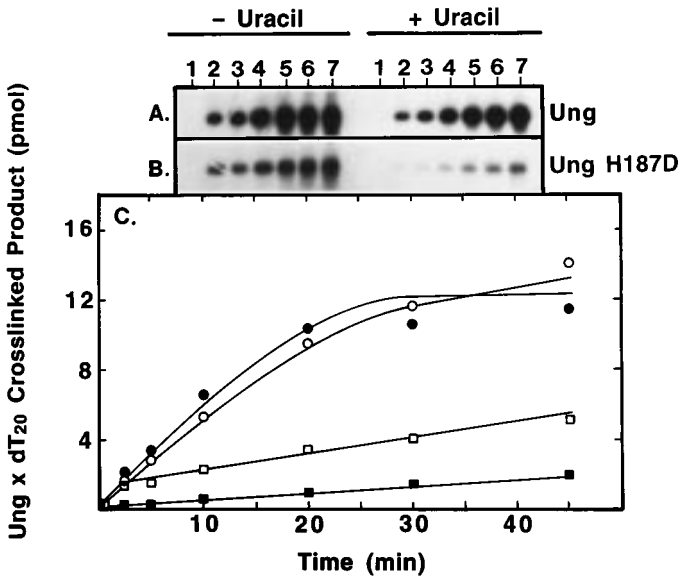


FIGURE 10: Effect of free uracil on UV-catalyzed cross-linking of Ung and Ung H187D to $dT_{20}$. (A) Two reaction mixtures (135 $\mu$L) containing 3.4 nmol of Ung, 6.8 nmol of [$^{32}$P]$dT_{20}$ and DAB buffer (pH 7.4) were irradiated with UV-light in the presence or absence of 2 mM uracil. Samples (15 $\mu$L) were removed after the irradiation times indicated below and subsequently analyzed by 12.5% SDS−PAGE as described under Materials and Methods. (B) An identical set of reactions were prepared except that 3.4 nmol of Ung H187D was substituted as the enzyme. Autoradiography was conducted to locate the cross-linked enzyme × [$^{32}$P]$dT_{20}$ species. Lanes 1−7 correspond to irradiation times of 0, 2.5, 5, 10, 20, 30, and 45 min, respectively. (C) The amount of enzyme × [$^{32}$P]$dT_{20}$ produced was quantitated by liquid scintillation counting as previously described for Ung (●) and Ung H187D (■) in the presence and Ung (○) and Ung H187D (□) in the absence of uracil.

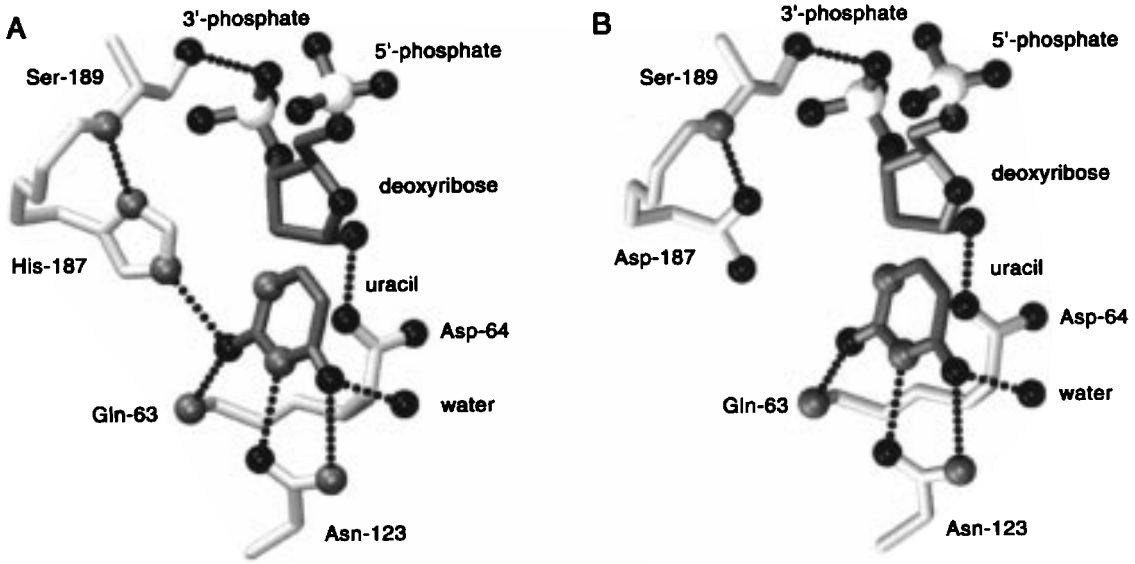


FIGURE 11: Model of *E. coli* Ung binding to uracil-containing DNA. The location of Ung (A) and Ung H187D (B) active site amino acid residues are shown as determined by high-resolution X-ray crystallography (*16*). The position of the cleaved uracil nucleotide was modeled into the uracil recognition pocket by superimposing the Ung structure onto the human uracil-DNA glycosylase:U/G-DNA cocrystal structure (*5*). Alignment was performed by the program CKWHENCE (*16*). The active-site residues portrayed are absolutely conserved between *E. coli* and human uracil-DNA glycosylase. The proposed interactions between various residues, uracil, deoxyribose phosphates, and water are indicated. Protein is shaded in light gray, DNA in dark gray; heteroatoms are nitrogen (gray), oxygen (black), and phosphorus (white).

substrate ($dT_{19}$−U) than to the abasic site-containing substrate ($dT_{19}$−AP) or even to the nonspecific substrate, $dT_{20}$. Since the turnover rate of Ung (800 uracils/min) is rapid compared to Ung H187D it might be expected that a significant fraction of uracil had been excised from $dT_{19}$−U during the UV irradiation reaction containing Ung. When human uracil-DNA glycosylase was cocrystallized with a 10 base double-stranded DNA containing either a U/A base pair or a U/G mismatch, free uracil and a deoxyribose C1′ OH were bound in the active site (*5*). Thus, it is conceivable that a portion of the Ung molecules cross-linked to a uracil base bound in the active site rather than to the thymine-DNA; such enzyme molecules may not be capable of binding DNA.

Addition of 2 mM uracil to the cross-linking reactions had no effect on the efficiency of Ung × $dT_{20}$ cross-linking, but the efficiency of Ung H187D × $dT_{20}$ cross-linking was reduced severalfold. These results demonstrated that the affinity of Ung was considerably greater for DNA than for uracil, as even 2 mM uracil did not disrupt Ung/$dT_{20}$ binding. These results show further that the His to Asp mutation has a greater affect on DNA affinity than on uracil binding,

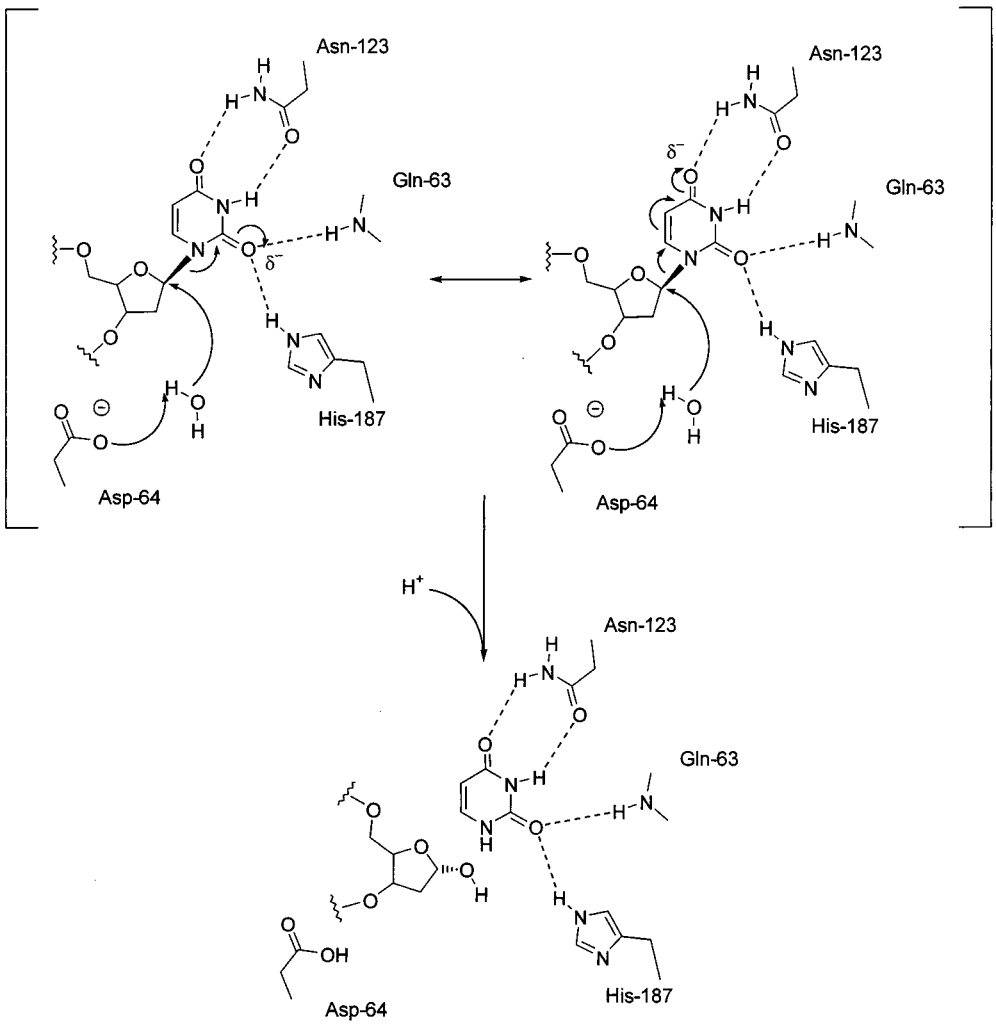


FIGURE 12: Scheme of the reaction mechanism for cleavage of the N1−C1′ glycosylic bond by *E. coli* Ung. Resonance forms of the proposed hydrolysis intermediates in the uracil-excision are illustrated. The N1−C1′ glycosylic bond is polarized by electron density withdrawal from the deoxyribose C1′ through N1 into the uracil ring. The developing negative charge is distributed about the uracil ring by resonance effects involving oxyanion formation at O2 and O4 and stabilized by hydrogen bonding with the side chains of His-187 and Asn-123, and the main-chain Gln-63 amide. The catalytic water is bound by Asp-64 in the water-activating loop formed by 64-Asp-Pro-Tyr-His-67 (*5*).

assuming that uracil bound in the active site prevents DNA binding.

On the basis of the collection of biochemical and structural data for *E. coli* Ung, we propose that His-187 participates in glycosylic bond scission as illustrated in Figure 12. Stable active-site geometry suggests that His-187 N$\delta$1 is a hydrogen bond acceptor to the Ser-189 main-chain amide. In the "closed" conformation, movement of the Leu intercalation loop (amino acid residues 187−195) brings the His-187 N$\epsilon$2 ~2 Å closer to the uracil O2 where it can act as a hydrogen bond donor (*4*, *5*, *16*), as previously suggested by Savva et al. (*14*). Delocalization of electron density across the His-187 imidazole side chain contributes to catalysis by stabilization of the oxyanion form of the uracil O2 carbonyl and the attendant polarization of the N1−C1′ glycosylic bond. The side chain of Asn-123 and the main chain of Gln-63 act to further stabilize electron delocalization in the uracil ring by forming hydrogen bonds with N3 and O4. In addition, we reason that the O4′ of the deoxyribose, because of its electron-withdrawing nature, also participates in forming a reactive, electrophilic C1′ since substitution of the less electronegative sulfur atom for O4′ resulted in a uracil nucleotide refractory to hydrolysis as reported by Parikh et al. (*5*). As observed in both the human (*4*, *5*) and the HSV-1 (*14*) uracil-DNA glycosylase structures, the side chain of the conserved Asp-64 appears properly positioned in *E. coli* Ung to bind the catalytic water (*15*, *16*). Electron density withdrawal from the deoxyribose C1′ renders the N1−C1′ bond vulnerable to nucleophilic attack by the water activated by the $\gamma$-carboxylate of Asp-64. In addition, the developing negative charge of the uracil base, stabilized by resonance effects and hydrogen bonding to active-site residues (Gln-63, Asn-123, and His-187), makes uracil a good leaving group. Abstraction of a proton from solvent by N1 also enhances uracil departure and restores electrostatic neutrality to the free uracil base following glycosylic bond scission.

The mechanism proposed here differs from previous proposals in several important respects. Recent structural information derived from the cocrystallization of human uracil-DNA glycosylase with uracil-DNA (*4*, *5*) shows that His-268 (Ung His-187) is on the wrong side of the uracil to carry out either a direct nucleophilic attack on C1′ or to mediate an indirect attack by serving as a general base to activate a nucleophilic water, as previously proposed (*18*). Unlike others (*14*), we propose that it is unnecessary to require protonation of uracil O2 in order to improve the

leaving group quality of the base. Rather, the developing negative charge that characterizes the transition state is not posited solely in the O2 oxyanion but is distributed among N1, O2, and O4 on the uracil ring by the effects of resonance and hydrogen bonding (Figure 11). The proximity of the Ser-189 NH to the His-187 imidazole N$\delta$1 in both open and closed conformations indicates that N$\delta$1 acts as a hydrogen bond acceptor to the main-chain amide; accordingly, the His-187 N$\epsilon$2 is a hydrogen bond donor to O2. In this scenario, it is unlikely that the His-187 imidazole binds two hydrogens, carries a full positive charge, and protonates O2 to return to electronic neutrality, as was proposed (*14*). The aromaticity of the imidazole side chain seems uniquely suitable to stabilize any partial charge associated with electrostatic interactions with the uracil nucleotide backbone and hydrogen bonding with uracil O2.

The relatively bulky nature of the imidazole side chain of His-187 may also contribute to the steric selectivity of the active site. This selectivity pocket is thought to distort the N1−C1′ glycosylic bond, since an intact extrahelical uracil residue in DNA does not easily "fit" into the active site without torsional strain (*5*, *16*). In contrast, the Asp-187 side chain is too small to contribute much to steric selectivity.

Substitution of Asp for His-187 has profound effects on the cleavage of the N1−C1′ glycosylic bond. Asp-187 does not extend far enough into the specificity pocket to allow a protonated side chain to hydrogen bond with uracil O2. On the other hand, it is too long to allow a water molecule to act as a bridge between the Asp-187 side-chain carboxylate and uracil O2 (*16*). In removing the hydrogen-bonding interaction of His-187 with uracil O2, the Asp-187 mutation not only hampers uracil binding but it also influences the stabilization of developing negative charge at O2 that is requisite for N1−C1′ bond cleavage. Simple removal of the hydrogen bond, as observed in the human H268L mutant, reduced the specific activity ~300-fold (*18*); however, the specific activity of the *E. coli* H187D mutant enzyme decreased an additional 2 orders of magnitude. The large effect of the Asp-187 mutation on specific activity most likely results from the destabilization of the hydrolytic transition state caused by electrostatic repulsion of the developing negative charge at uracil O2 by the Asp-187 carboxylate. Reduction of this electrostatic repulsion by partial protonation of the Asp-187 side chain may be the fundamental influence that shifts the pH optimum of the mutant enzyme from 8.0 to 7.0. Hence, the Asp-187 mutation provides a subtle probe of the Ung reaction mechanism, indicating how an amino acid residue whose side chain is ~4.5 Å from the nearest atom of the scissile bond can reduce the reaction rate by ~55000-fold.

In summary, we propose that the imidazole side chain of Ung His-187 (1) facilitates uracil nucleotide flipping by "pulling" the uracil residue into the active site through favorable electrostatic interactions with the 3′- and 5′-uracil deoxyribose phosphates; (2) contributes sterically to the fit and selectivity of the uracil binding pocket; and (3) stabilizes the hydrolytic transition state by hydrogen bonding with uracil O2. The reaction mechanism advanced here provides a realistic explanation of the properties of the Ung H187D mutant enzyme. However, how the release of the uracil-excision reaction products, free uracil, and AP-site DNA affects the catalytic efficiency of uracil-DNA glycosylase remains to be established.

## REFERENCES


1. Krokan, H. E., Standal, R., and Slupphaug, G. (1997) *Biochem. J. 325*, 1−16.
2. Mosbaugh, D. W., and Bennett, S. E. (1994) *Prog. Nucleic Acid Res. Mol. Biol. 48*, 315−370.
3. Lindahl, T., Ljungquist, S., Siegert, W., Nyberg, B., and Sperens, B. (1977) *J. Biol. Chem. 252*, 3286−3294.
4. Slupphaug, G., Mol, C. D., Kavli, B., Arvai, A. S., Krokan, H. E., and Tainer, J. A. (1996) *Nature 384*, 87−92.
5. Parikh, S. P., Mol, C. D., Slupphaug, G., Bharati, S., Krokan, H. E., and Tainer, J. A. (1998) *EMBO J. 17*, 5214−5226.
6. Kunkel, T. A., and Wilson, S. H. (1996) *Nature 384*, 25−26.
7. Bennett, S. E., Sanderson, R. J., and Mosbaugh, D. W. (1995) *Biochemistry 34*, 6109−6119.
8. Higley, M., and Lloyd, R. S. (1993) *Mutat. Res. 294*, 109−116.
9. Varshney, U., Hutcheon, T., and van de Sande, J. H. (1988) *J. Biol. Chem. 263*, 7776−7784.
10. Bennett, S. E., Jensen, O. N., Barofsky, D. F., and Mosbaugh, D. W. (1994) *J. Biol. Chem. 269*, 21870−21879.
11. Domena, J. D., Timmer, R. T., Dicharry, S. A., and Mosbaugh, D. W. (1988) *Biochemistry 27*, 6742−6751.
12. Olsen, L. C., Aasland, R., Wittwer, C. U., Krokan, H. E., and Helland, D. E. (1989) *EMBO J. 8*, 3121−3125.
13. Upton, C., Stuart, D. T., and McFadden, G. (1993) *Proc. Natl. Acad. Sci. U.S.A. 90*, 4518−4522.
14. Savva, R., McAuley-Hecht, K., Brown, T., and Pearl, L. (1995) *Nature 373*, 487−493.
15. Ravishankar, R., Bidya Sagar, M., Roy, S., Purnapatre, K., Handa, P., Varshney, U., and Vijayan, M. (1998) *Nucleic Acids Res. 26*, 4880−4887.
16. Putnam, C. D., Shroyer, M. J. N., Lundquist, A. J., Mol, C. D., Arvai, A. S., Mosbaugh, D. W., and Tainer, J. A. (1999) *J. Mol. Biol. 287*, 331−346.
17. Mol, C. D., Arvai, A. S., Sanderson, R. J., Slupphaug, G., Kavli, B., Krokan, H. E., Mosbaugh, D. W., and Tainer, J. A. (1995) *Cell 82*, 701−708.
18. Mol, C. D., Arvai, A. S., Slupphaug, G., Kavli, B., Alseth, I., Krokan, H. E., and Tainer, J. A. (1995) *Cell 80*, 869−878.
19. McGeoch, D. J., Dalrymple, M. A., Davison, A. J., Dolan, A., Frame, M. C., McNab, D., Perry, L. J., Scott, J. E., and Taylor, P. (1988) *J. Gen. Virol. 69*, 1531−1574.
20. Worrad, D. M., and Caradonna, S. (1988) *J. Virol. 62*, 4774−4777.
21. Lundquist, A. J., Beger, R. D., Bennett, S. E., Bolton, P. H., and Mosbaugh, D. W. (1997) *J. Biol. Chem. 272*, 21408−21419.
22. Bennett, S. E., Schimerlik, M. I., and Mosbaugh, D. W. (1993) *J. Biol. Chem. 268*, 26879−26885.
23. Caradonna, S., Ladner, R., Hansbury, M., Kosciuk, M., Lynch, F., and Muller, S. (1996) *Exp. Cell. Res. 222*, 345−359.
24. Kunkel, T. A., Roberts, J. D., and Zakour, R. A. (1987) *Methods Enzymol. 154*, 367−382.
25. Bennett, S. E. (1995) *Thesis*, Oregon State University, Corvallis, Oregon.
26. Sanger, F., Nicklen, S., and Coulson, A. R. (1977) *Proc. Natl. Acad. Sci. U.S.A. 74*, 5463−5467.
27. Sanderson, R. J., and Mosbaugh, D. W. (1996) *J. Biol. Chem. 271*, 29170−29181.
28. Bennett, S. E., and Mosbaugh, D. W. (1992) *J. Biol. Chem. 267*, 22512−22521.
29. Molnar, G., O'Leary, N., Pardee, A. B., and Bradley, D. W. (1995) *Nucleic Acids Res. 23*, 3318−3326.
30. Laemmli, U.K. (1970) *Nature 227*, 680−685.
31. Bradford, M. M. (1976) *Anal. Biochem. 72*, 248−254.
32. Savva, R., and Pearl, L. H. (1995) *Nat. Struct. Biol. 2*, 752−757.
33. Panayotou, G., Brown, T., Barlow, T., Pearl, L. H., and Savva, R. (1998) *J. Biol. Chem. 273*, 45−50.


BI982986J